

Late stages in the ordering of magnetic skyrmion lattices

James Stidham^{1,2} and Michel Pleimling^{1,2,3}

¹*Department of Physics, Virginia Tech, Blacksburg, VA 24061-0435, USA*

²*Center for Soft Matter and Biological Physics,*

Virginia Tech, Blacksburg, VA 24061-0435, USA

³*Academy of Integrated Science, Virginia Tech, Blacksburg, VA 24061-0563, USA*

(Dated: January 13, 2022)

Abstract

The late-stage ordering of interacting magnetic skyrmions is studied numerically through extensive Langevin molecular dynamics simulations. Defining skyrmion displacements that change the connectivity of cells obtained in a Voronoi tessellation as events, we investigate event histograms as a function of the time elapsed since preparing the system as well as the histograms of consecutive events as a function of the time separating these two events. These histograms, which provide unique insights into the transient properties during the ordering process of skyrmion matter, show a characteristic behavior that allows the Magnus-force dominated regime, where the Magnus force accelerates the relaxation process, to be distinguished from the noise-dominated regime, where the Magnus force enhances the effects of thermal noise. In the Magnus-force dominated regime the different histograms display power-law tails with exponents that depend on the strength of the Magnus force.

I. INTRODUCTION

Since their first experimental realizations^{1,2} and, especially, since their observation at room temperature³⁻⁵, arrangements of magnetic skyrmions, nanometer sized particlelike spin textures^{6,7}, have attracted much attention⁸. Racetrack memory devices⁹⁻¹¹ and logic gates¹² are some of the possible promising applications of these spin textures.

One of the characteristic features of skyrmions is the presence of the nondissipative Magnus force. As this force acts perpendicular to the skyrmion's velocity, it has a major effect on the dynamics of the spin textures, especially in cases where skyrmions are not isolated, but interact with each other and/or with defects. Intriguing new phenomena can emerge under these circumstances. For example, in driven systems a constant angle, known as the skyrmion Hall angle, appears between the direction of the drive and the direction of displacement^{7,13-19}. Other studies have focused on the appearance of avalanches when the driven skyrmions interact with random pins²⁰, the pattern formation of geometrically confined skyrmions²¹, the existence of nonequilibrium phase transitions between different dynamic phases^{22,23}, shear banding of driven skyrmions in inhomogeneous pinning arrays²⁴, laning transitions in presence of damping²⁵, as well as the formation of skyrmion crystals^{26,27} and the flow of skyrmion lattices²⁸.

Intriguingly, randomly nucleated skyrmions may be subjected to thermal fluctuations²⁹⁻³¹ and undergo a relaxing process. Some aspects of the ordering of interacting skyrmions has been investigated through Langevin molecular dynamics^{32,33} simulations and has also been observed recently in experiments using sub-nm thick CoFeB-based multilayer systems³⁴. These studies have revealed that the interplay between repulsive skyrmion-skyrmion interaction, Magnus force, and thermal noise yields different dynamic regimes. In the Magnus-force dominated regime that prevails for weak thermal noise, the Magnus force cooperates with the repulsive skyrmion-skyrmion interaction and accelerates the relaxation to the triangular lattice. Strong thermal noise yields the noise-dominated regime that is characterized by the fact that the Magnus force amplifies the effects of the thermal noise so that the dynamics is noisier than in absence of this nondissipative force. Even richer scenarios are possible in situations where the mobility of skyrmions is affected by pinning that stems from material imperfections³⁵⁻⁴⁰. Whereas collective pinning due to strong attractive defects can yield a skyrmion glass⁴¹, pinning is reduced for weaker pinning strengths as the Magnus force helps

skyrmions avoid caging effects by bending around defects³³.

The aim of the present work is to provide an in-depth view of the ordering process of interacting skyrmions in situations dominated by the Magnus force and / or thermal noise. Whereas in Ref.³² the emphasis was on the early stages of the ordering process, including a possible aging scaling regime, in this study we also investigate the later stages where only a few defects persist in an otherwise well ordered skyrmion lattice. Our study, which to our knowledge encompasses the first systematic numerical investigation of the relaxation processes in the late-time dynamic regime before the system reaches equilibrium, highlights the usefulness of event statistics in the context of skyrmion matter. In order to monitor this ordering process, we consider at every timestep a Voronoi tessellation of the skyrmion system and count the number of cells that have six edges. We then define as events skyrmion displacements that change the number of cells with six edges. In the late stages of the process, these events are rare and a large amount of timesteps separate consecutive events. Our analysis is based on histograms of the number of events that have taken place since preparing the system as well as on histograms of the number of consecutive events that take place within a given time interval. We show that these histograms not only allow us to identify the different dynamic regimes, they also are characterized in the Magnus-force dominated regime by algebraic tails governed by exponents whose values depend on the strength of the Magnus force. For weak noise these exponents are found to not depend on the noise strength.

In the next Section, we first review the particle-based model⁴² used for our Langevin molecular dynamics simulations. We also discuss in more detail the quantities that we investigate in our work. In Section III, we first present results without thermal noise, thus focusing exclusively on the Magnus-force dominated regime. We then add thermal noise and show that this leads to different dynamic regimes. The final Section presents our conclusions.

II. MODEL AND QUANTITIES

We follow previous work³² and consider a particle-based model⁴² of interacting skyrmions moving on a two-dimensional surface. The rigid structure approximation underlying the model is valid in the low-density regime^{7,16,43}. In this description, skyrmions interact via a long-range repulsive force and are subjected to the velocity-dependent Magnus force. The

skyrmions can be driven by an electrical field and can interact with defects. In this paper, we focus on ordering processes taking place in the absence of an external drive and in situations where skyrmion-defect interactions can be omitted. Following Thiele's approach⁴⁴, the system is then modeled as a set of Langevin equations for the skyrmion drift velocities:

$$\eta \mathbf{v}_i = \beta \hat{\mathbf{z}} \times \mathbf{v}_i + \mathbf{F}_i^s + \mathbf{f} \quad (1)$$

where the N_s different skyrmions are labeled by the index $i = 1, \dots, N_s$, whereas η is the damping coefficient. The first term on the right hand side is the nondissipative Magnus force with strength β , acting in the direction perpendicular to the velocity. The presence of this force, which results in curved trajectories, has a significant impact on the dynamic properties of interacting skyrmions, especially far from stationarity^{32,33}. We impose the constraint $\eta^2 + \beta^2 = 1$ from which follows that the average velocity magnitude of a free skyrmion is not dependent on the Magnus force. We focus on the following values of the ratio $\alpha = \beta/\eta$ of the Magnus force strength and the damping coefficient: $\alpha = 0$, i.e. no Magnus force, $\alpha = 5$, and $\alpha = 9.962$, which is a realistic value for MnSi^{42,45}. \mathbf{F}_i^s denotes the resultant force on skyrmion i due to the presence of the other skyrmions: $\mathbf{F}_i^s = \sum_{j \neq i} K_1(r_{ij}/\xi) \hat{\mathbf{r}}_{ij}$ with the modified Bessel function of the second kind K_1 ⁴², the healing length ξ (we choose units such that the healing length $\xi = 1$), and the unit vector $\hat{\mathbf{r}}_{ij} = \mathbf{r}_{ij}/r_{ij} = (\mathbf{r}_i - \mathbf{r}_j)/|\mathbf{r}_i - \mathbf{r}_j|$ pointing from skyrmion j to skyrmion i . For large distances, $r_{ij}/\xi \gg 1$, this force decays exponentially. In our Langevin dynamics simulations we use a cut-off length λ with typically $\lambda = 7\xi$ (see also inset in Fig. 3). Finally, the last term in Eq. (1) describes delta-correlated thermal white noise with mean 0: $\langle f_\mu(t) \rangle = 0$ and $\langle f_\mu(t) f_\nu(t') \rangle = \sigma^2 \delta_{\mu\nu} \delta(t - t')$, with $\sigma^2 = 2\eta k_B T$.

The two-dimensional systems we discuss in the following typically have the size $\frac{2}{\sqrt{3}}L \times L$ with $L = 72$ in units of skyrmion radii, but we also considered systems with $L = 36$ in order to discuss finite-size effects. The combination of this shape and periodic boundary conditions allow the skyrmions in absence of thermal noise to settle into a triangular lattice at equilibrium. The skyrmion density we choose was 10%, which results in systems containing 596 skyrmions.

Initially, at time $t = 0$, we randomly distribute the skyrmions in the domain, where we make sure that skyrmions are not overlapping. The equations of motion (1) are then solved with a standard fourth-order Runge-Kutta method and the integration timestep $dt = 0.01$. In the absence of external drive and defects that can pin the skyrmions, the skyrmions un-

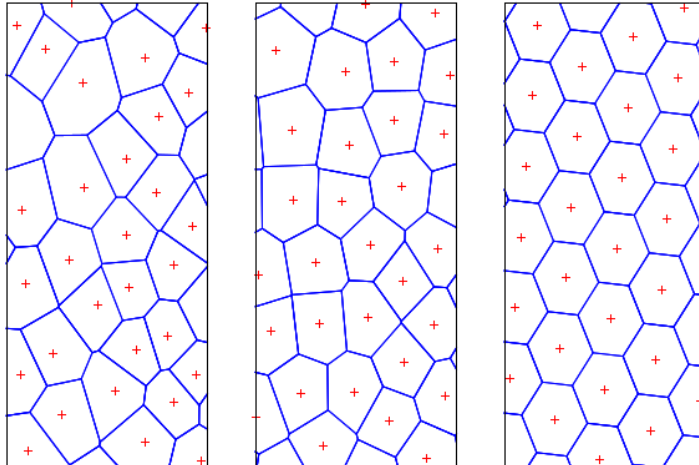


FIG. 1: Part of a skyrmion lattice at different times since preparing the system in a disordered initial state. From left to right: $t = 100$, $t = 1,000$, and $t = 10,000$. The skyrmion positions are indicated by the red marks. The lines result from the Voronoi tessellations. In the perfect ordered triangular lattice all polygons have six edges. The values of the system parameters are $L = 36$, $\lambda = 7\xi$, $\alpha = 9.962$, and $\sigma = 0$.

dergo an ordering process and relax towards an (in presence of weak noise approximately) ordered triangular lattice. In the absence of noise and in the large-volume limit the system will not display perfect long-range order, in agreement with the Hohenberg-Mermin-Wagner theorem. However, our systems are so small that a hexatic phase can not be distinguished from a crystalline phase. A convenient way to assess the level of ordering is through Voronoi tessellation that readily reveals local ordering in an (approximate) hexagonal structure through the appearance of six-sided cells, whereas in regions with defects in the hexagonal structure, cells with more or less than six edges persist^{32,33}. Starting from a disordered state, the Voronoi tessellation initially yields a mixture of oddly-shaped cells with variable numbers of edges. As time progresses and the skyrmions start to order in a hexagonal structure, six-sided cells quickly prevail, with the exception of long lasting defects that manifest themselves through persisting pairs of cells where one has five and the other seven edges. The configurations shown in Fig. 1 illustrate this relaxation process.

In relaxation and ordering processes different dynamic regimes can be identified⁴⁶ when comparing the time elapsed since preparing the system with both the microscopic time scale t_{micro} and the equilibration time t_{eq} . In the early regime, with $t \gtrsim t_{micro}$, the system remains

in quasi-equilibrium in a state close to the state of initial preparation before passing into the aging regime. In the aging or intermediate regime, times are much larger than microscopic times, but much smaller than the equilibration time: $t_{micro} \ll t \ll t_{eq}$. It is in this regime where dynamical (aging) scaling may be encountered, often as a result of an algebraically increasing unique length that characterizes the system^{32,33}. Finally, for very long times with $t \lesssim t_{eq}$ the typical length saturates and approaches a maximum value as the system approaches equilibrium.

In this publication, in contrast to previous work on interacting skyrmion systems that mainly investigated the early stages^{32,33} of the ordering process, we focus on the late stages where most skyrmions are in stable positions, with a few remaining defects. Our analysis is based on event statistics where we define an event as a change in the number of Voronoi cells with six edges. This is achieved by computing two different histograms. For the first histogram we record the time t (measured since the initial preparation of the system) at which an event happens and increase by one the counter $\tilde{N}(t)$ that counts the number of events happening at time t since preparing the system. We build a histogram by performing many (between 1,000 and 10,000) simulations. The quantity shown in the figures is then the ensemble averaged number of events per skyrmion at time t : $N(t) = \tilde{N}(t)/(N_s n_{runs})$ where n_{runs} is the total number of independent runs. For the second histogram we measure the time Δt separating two consecutive events and increase by one the counter $\tilde{M}(\Delta t)$ that counts the number of events separated by the time interval Δt . Again, we discuss in the following a normalized histogram that is both ensemble and skyrmion averaged: $M(t) = \tilde{M}(t)/(N_s n_{runs})$.

It is convenient to bin the data in order to provide smoother curves. For the figures discussed in the following, we use a bin size of 200 timesteps for the number N of events per skyrmion, whereas for the number M of consecutive events separated by a fixed time interval, the bin size is 20. We checked that other bin sizes do not change any of our conclusions.

While our emphasis has been on event statistics and normalized histograms, we have also computed at different times the pair correlation function

$$g(r) = \sum_{i=1}^{N_s} \sum_{i \neq j} \delta(r - r_{ij}) / (2\pi r dr \rho N_s) \quad (2)$$

with the skyrmion density $\rho = 0.1$ and the thickness $dr = 0.1$ of the ring with radius r . As the envelop of $g(r) - 1 \sim e^{-r/\varepsilon(t)}$, we can extract from this quantity the time-dependent

correlation length $\varepsilon(t)$.

III. RESULTS

It is our goal to gain a qualitative and quantitative understanding of the effects the Magnus force has on the later-time ordering behavior of a system of interacting skyrmions. Earlier studies at intermediate times have revealed^{32,33} the presence of two different relaxation regimes, depending on the relative strengths of the Magnus force and the thermal noise. For weak (or absent) thermal noise, we are dealing with the Magnus-force dominated regime that is characterized by a Magnus force induced acceleration of the relaxation towards the triangular lattice. For strong thermal noise, however, the Magnus force further enhances the effect of the noise when compared to a system that relaxes without this force being present. In order to disentangle these two effects, we consider in the following first the case without thermal noise before discussing the more general situation where both Magnus force and thermal noise are present.

Events being defined as changes of skyrmion positions that result in some of the Voronoi cells changing their number of edges, these events provide a reasonable proxy for the time-dependent ordering process. The discussion of event statistics will therefore provide insights into the late stages of the ordering of interacting skyrmion systems.

A. Systems without thermal noise

We start our discussion with Fig. 2 that shows the ensemble averaged number of events per skyrmion as a function of the time elapsed since preparing the system. The three curves correspond to three different values of the ratio of the Magnus force strength and the damping coefficient studied in this work.

We first note that in the short- and medium-time regimes, the number of events increases with increasing Magnus force. This is a manifestation of the already mentioned accelerating effect the Magnus force has on the ordering process in the absence of noise. Already, a small value of α accelerates relaxation, compare the green line with $\alpha = 5$ to the black line with $\alpha = 0$. Additional strengthening of the Magnus force mainly results in minor changes. Independently of the value of α , all three curves in Fig. 2 exhibit power-law tails. This is

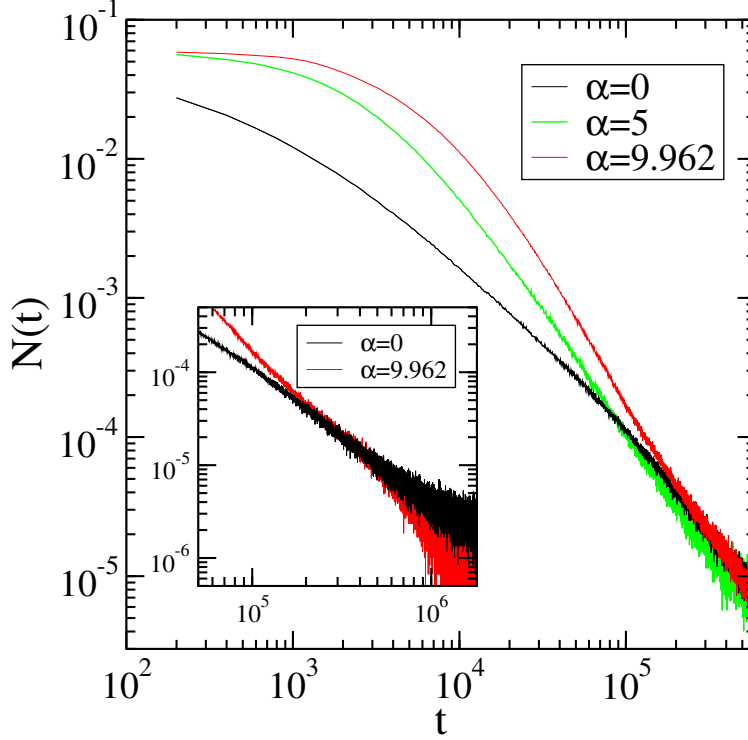


FIG. 2: Number N of events per skyrmion as a function of the number of time steps t since preparation of the system in a disordered initial state. Data are shown for different strengths of the Magnus force α . The inset highlights that with Magnus force the long-time algebraic decay is governed by a different exponent than without this force. The system parameters are $L = 72$, $\lambda = 7\xi$, and $\sigma = 0$, i.e. thermal noise is absent. The data result from an average over at least 5,000 independent runs.

reminiscent of the fat tails found in processes with rare events⁴⁷ and indicates that in the late-time regime, the rare displacements of skyrmions large enough to change the shape of Voronoi cells are algebraically distributed in time. We find that the exponent governing this decay depends on the strength of the Magnus force, see inset in Fig. 2: without the Magnus force, we have the value $-1.42(3)$, for $\alpha = 5$ the value is $-1.60(2)$, whereas for $\alpha = 9.962$ we obtain the value $-1.75(2)$. This increase of the magnitude of the exponent is consistent with the expectation that for larger values of α , relaxation is faster, yielding a higher degree of order and, concomitantly, fewer events at a fixed large time since preparation of the system.

Fig. 3 illustrates the dependence of the number of events per skyrmion on two key system parameters: the system size L in the main figure and the cut-off length λ in the inset. Reducing the system size L decreases the equilibration time. The final approach

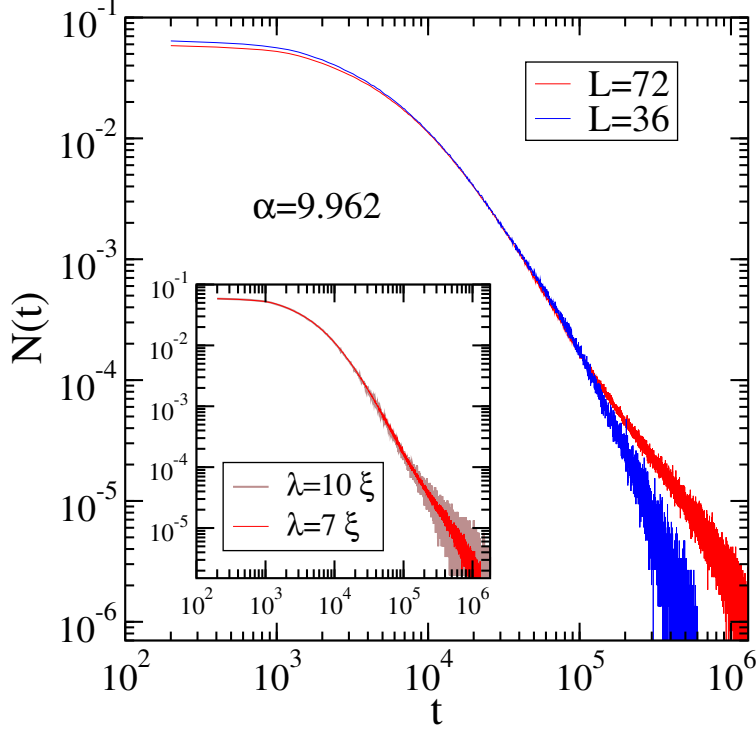


FIG. 3: System size dependence of the number N of events per skyrmion as a function of the number of time steps t for systems with the Magnus force strength $\alpha = 9.962$. The systems have been prepared initially in a disordered state. The inset shows how N changes for $L = 72$ when the cut-off length λ is changed from 7ξ to 10ξ . These data, which have been obtained in absence of thermal noise, result from an average over 1,000 independent runs for $\lambda = 10\xi$ and 10,000 independent runs for $\lambda = 7\xi$.

to equilibrium is revealed by deviations from a power-law behavior of N , and a transition to a more exponential relaxation stage (see the data for $L = 32$). As shown in the inset, increasing the cut-off length λ (in the figure from 7 skyrmion radii to 10 skyrmion radii) increases the noise in the ensemble averaged data and makes it harder to obtain reliable data for large times t , but does otherwise not affect the relaxation process.

We also analyzed how the number M of consecutive events changes as a function of the time Δt elapsed between these two consecutive events, see Fig. 4. For large separation times between consecutive events, M decays algebraically, and this is both in the presence and the absence of a Magnus force. The strength of the Magnus force impacts the exponent of the algebraic decay in a similar way as for the quantity N : the system orders quicker for a larger Magnus force, and the probability of encountering two consecutive events separated by a

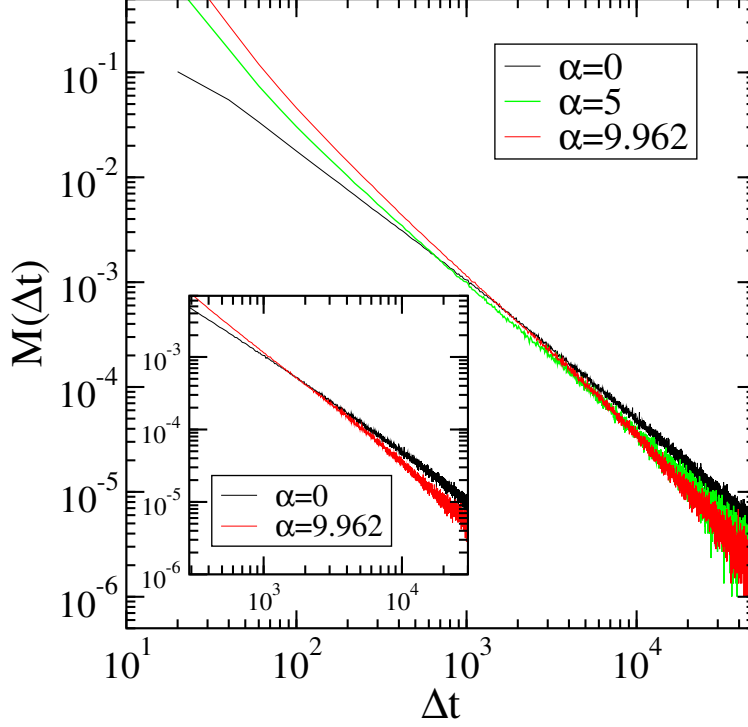


FIG. 4: Number M of consecutive events per skyrmion separated by a fixed number of time steps Δt . Data are shown for different strengths of the Magnus force α . The inset highlights that with the Magnus force, the algebraic decay of this quantity for large separating times is governed by a different exponent than without this force. The system parameters are $L = 72$, $\lambda = 7\xi$, and $\sigma = 0$, i.e. thermal noise is absent. The data result from an average over at least 5,000 independent runs. All the systems have been prepared initially in a disordered state.

large time difference is reduced. This is captured in the values of the power-law exponent: $-1.56(1)$ without Magnus force, whereas with Magnus force we have $-1.75(2)$ for $\alpha = 5$ and $-1.84(3)$ for $\alpha = 9.962$. Additional differences between the cases with and without Magnus force also show up for small separation times between consecutive events, as the quicker relaxation in presence of the Magnus force results in a larger number of events that happen close together.

Fig. 5 shows that the pair correlation function (2) evolves as a function of time, as expected for a system out of equilibrium that undergoes an ordering process. The envelop of $g(r) - 1$ displays an exponential decay as a function of distance r . The correlation length extracted from the exponentially decaying envelop is shown in the inset of Fig. 5 in presence and in absence of the Magnus force. Focusing on the intermediate and late-

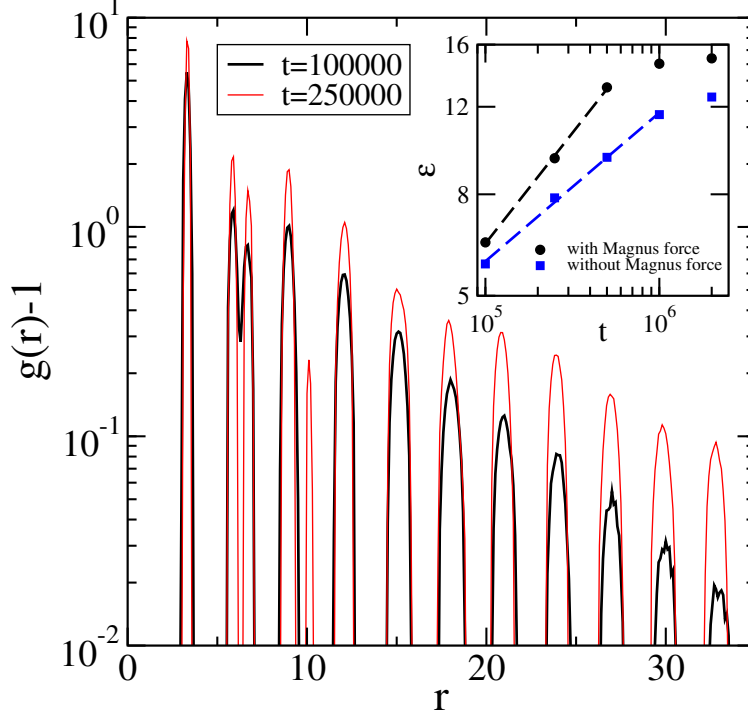


FIG. 5: Pair correlation function $g(r)$ as a function of distance r for two different times with the Magnus force but without noise. Plotting $g(r) - 1$ in a linear-log plot shows that the envelop decays exponentially with a time-dependent correlation length $\varepsilon(t)$. The inset compares the correlation lengths with and without Magnus force in absence of noise. The dashed lines are power-law fits with exponents 0.44 for the case with Magnus force, whereas without Magnus force the exponent is 0.30. The system parameters are $L = 72$, $\lambda = 7\xi$, and $\sigma = 0$, i.e. thermal noise is absent. The data result from an average over 500 independent runs. All the systems have been prepared initially in a disordered state.

time regimes, we see that the correlation length increases algebraically with time in the intermediate regime, with an exponent 0.44 in presence of the Magnus force that is larger than the exponent 0.30 obtained in absence of the Magnus force. This again highlights that the Magnus force accelerates the ordering process, as revealed by a larger power-law exponent, and a subsequent earlier crossover to the late-time non-algebraic growth regime. These findings are similar to those obtained earlier³² for the time-dependent average nearest-neighbor distance, with the notable exception that the deviation of $\varepsilon(t)$ from a power law is more gradual, which allows an easier determination of the growth exponent.

B. Systems with thermal noise

The effect of noise on the relaxation process is shown in Figures 6 and 7. Inspection of these two figures reveals a variety of aspects that need to be mentioned. In general, adding noise results in increasing the total number of events at a given time since preparation of the system. Particles are more mobile due to the random kicks received because of thermal noise which results in an overall increase of skyrmion displacements that change the number of edges of some cells. In absence of the Magnus force, see Fig. 6a, already a small value of the noise strength yields pronounced deviations from the $\sigma = 0$ data. For $\alpha = 9.962$, however, the same noise level results in only minor modifications, as shown in Fig. 6b. A strong Magnus force and the resulting curved trajectories of the skyrmions diminish the effects of weak random kicks. For large noise strengths, as for example $\sigma = 1$ in the figure (blue lines), the reverse situation is encountered, with the noise having a more pronounced effect in presence of the Magnus force. Indeed, for $\sigma = 1$ we are in the noise-dominated regime^{32,33} where the Magnus force enhances the effects coming from thermal noise. Consequently, in Fig. 6b, the number of events per skyrmions is, to a large extent, independent of the time since preparing the system, see blue line. This is different in Fig. 6a for $\alpha = 0$ and $\sigma = 1$, where a slow ordering process persists that results in a slow decrease of the blue line.

We note that for small noise strengths $\sigma \leq 0.1$ the algebraic decay at large values of t is largely independent of the noise strength, yielding values for the exponent that are consistent with those obtained for $\sigma = 0$, both in the absence and presence of the Magnus force. The much enhanced noise in the data makes a precise measurement of the exponent in presence of thermal noise difficult.

The curves shown in Fig. 7 for the number of consecutive events per skyrmion for a fixed time difference provide a complementary view of the effects of thermal noise. This quantity also reveals the reduced impact that weak thermal noise has on the ordering process in the presence of the Magnus force, including the fact that the exponents of the power-law decay are not changed when adding weak noise. For strong thermal noise, two consecutive events separated by more than a hundred timesteps are not encountered in the presence of the Magnus force, see Fig. 7b, which again highlights that the Magnus force reinforces the disordering effect of strong thermal noise.

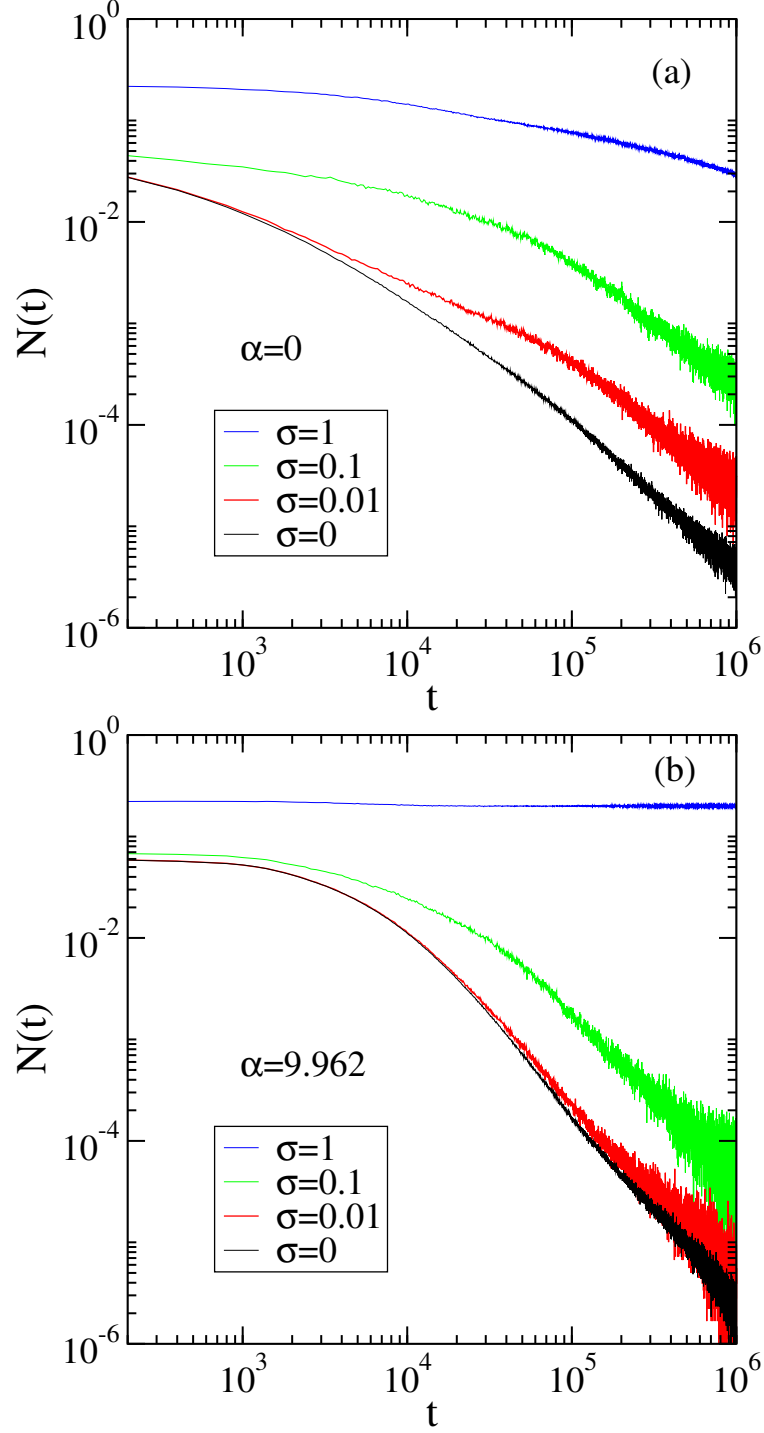


FIG. 6: Number N of events per skyrmion as a function of the number of time steps t for various strengths of the thermal noise. (a) Systems without Magnus force, (b) systems with a Magnus force of strength $\alpha = 9.962$. Other system parameters are set at $L = 72$ and $\lambda = 7\xi$. The data are the average of at least 1,000 independent runs.

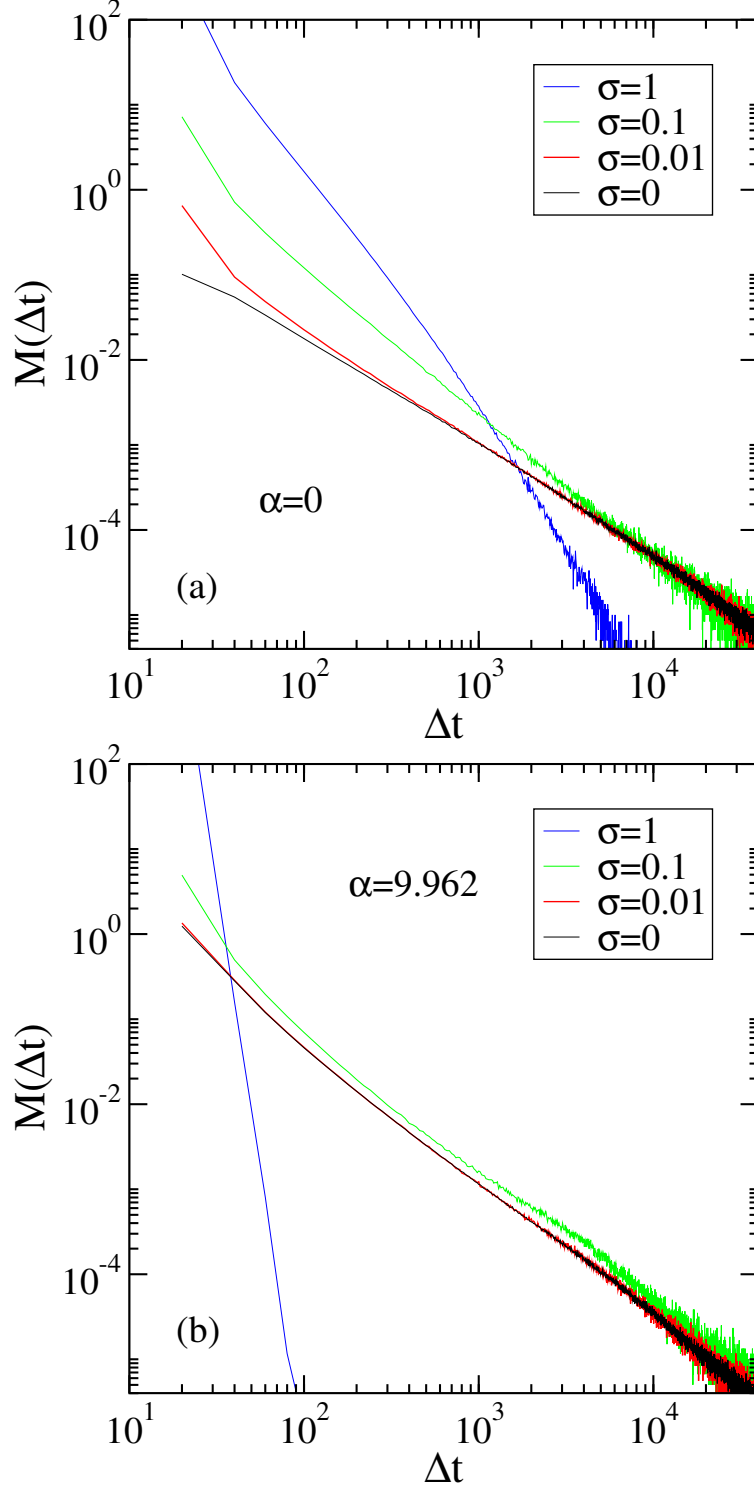


FIG. 7: Number M of consecutive events per skyrmion separated by a fixed number of time steps Δt for various strengths of the thermal noise. (a) Systems without Magnus force, (b) systems with a Magnus force of strength $\alpha = 9.962$. Other system parameters are set at $L = 72$ and $\lambda = 7\xi$. The data are the average of at least 1,000 independent runs.

IV. CONCLUSION

Up to now the systematic numerical investigation of the dynamic relaxation processes in interacting skyrmion systems have been restricted to the aging scaling regime encountered at intermediate times^{32,33}, i.e. at times that are large compared to microscopic time scales but small compared to the equilibration time. This work presents, to our knowledge for the first time, an analysis of the properties of skyrmion matter at late stages of the ordering process, where skyrmion displacements that enhance locally ordering happen rarely. In order to gain insights into this late-stage relaxation process, we propose to apply event statistics to skyrmion systems.

The Magnus force, a velocity dependent force that acts perpendicular to the direction of propagation and therefore yields curved trajectories, has a major impact on ordering processes taking place in systems of interacting skyrmions^{32,33}. In the absence of external drive, one identifies two different dynamic regimes, depending on the relative strengths of the Magnus force and the thermal noise. For weak thermal noise, the system is in the Magnus-force dominated regime where the Magnus force yields an acceleration of the ordering process when compared to the case without the Magnus force. The noise-dominated regime prevails for strong thermal noise and is characterized by the fact that the Magnus force enhances the disordering effects of the noise.

In this paper, we have focused on the ordering process of skyrmion matter without external drive and in situations where interactions with pinning defects can be neglected. Through the study of the number of events (defined as rearrangements that change the edge numbers of some cells obtained through Voronoi tessellation) at a fixed time since preparing the systems, as well as of the number of consecutive events happening for a fixed time interval, interesting information on the relaxation process are obtained. The two dynamic regimes yield a characteristic behavior of these quantities that can easily be identified. In the noise-dominated regime, both quantities display power-law decays governed by exponents whose values depend on the strength of the Magnus force. Interestingly, these exponents are found to be unchanged in the presence of weak noise, so that the counting of events as defined in this work may provide a possible way to investigate the different dynamic regimes in experimental settings as those discussed recently in³⁴.

In cases where external drive and / or pinning defects are present, more complicated

dynamic scenarios are encountered away from stationarity. For example, strong attractive pins can capture a substantial fraction of the skyrmions, which then results in caging effects for the remaining skyrmions due to the repulsive skyrmion-skyrmion interactions³³. We expect that in this and related scenarios the number of events per skyrmion obtained from a Voronoi tessellation displays complicated, but characteristic, features that are worth studying in the future.

Acknowledgments

This material is based upon work supported by the U.S. Department of Energy, Office of Science, Office of Basic Energy Sciences, Division of Materials Sciences and Engineering under Award Number DE-SC0002308. We thank Uwe C. Täuber for a useful discussion.

-
- ¹ S. Mühlbauer, B. Binz, F. Jonietz, C. Pfleiderer, A. Rosch, A. Neubauer, R. Georgii, and P. Böni, *Science* **323**, 915 (2005).
 - ² X. Z. Yu, Y. Onose, N. Kanazawa, J. H. Park, J. H. Han, Y. Matsui, N. Nagaosa, and Y. Tokura, *Nature (London)* **465**, 901 (2010).
 - ³ S. Woo, K. Litzius, B. Krüger, M.-Y. Im, L. Caretta, K. Richter, M. Mann, A. Krone, R. M. Reeve, M. Weigand, P. Agrawal, I. Lemesch, M.-A. Mawass, P. Fischer, M. Kläui, and G. S. D. Beach, *Nat. Mater.* **15**, 501 (2016).
 - ⁴ O. Boulle, J. Vogel, H. Yang, S. Pizzini, D. de Souza Chaves, A. Locatelli, T. O. Mentes, A. Sala, L. D. Buda-Prejbeanu, O. Klein, M. Belmeguenai, Y. Roussigné, A. Stashkevich, S. M. Chérif, L. Aballe, M. Foerster, M. Chshiev, S. Auffret, I. M. Miron, and G. Gaudin, *Nat. Nanotechnol.* **11**, 449 (2016).
 - ⁵ R. D. Desautels, L. DeBeer-Schmitt, S. A. Montoya, J. A. Borchers, S.-G. Je, N. Tang, M.-Y. Im, M. R. Fitzsimmons, E. E. Fullerton, D. A. Gilbert, *Phys. Rev. Mat.* **3** 104406 (2019).
 - ⁶ U. K. Rößler, A. N. Bogdanov, and C. Pfleiderer, *Nature (London)* **442** 797 (2006).
 - ⁷ N. Nagaosa and Y. Tokura, *Nat. Nanotechnol.* **8**, 899 (2013).
 - ⁸ C. Back, V. Cros, H. Ebert, K. Everschor-Sitte, A. Fert, M. Garst, T. Ma, S. Mankovsky, T. L. Monchesky, M. Mostovoy, N. Nagaosa, S. S. P. Parkin, C. Pfleiderer, N. Reyren, A. Rosch, Y.

- Taguchi, Y. Tokura, K. von Bergmann, and J. Zang, arXiv:2001.00026 and J. Phys. D: Appl. Phys. in press.
- ⁹ A. Fert, V. Cros, and J. Sampaio, Nat. Nanotechnol. **8**, 152 (2013).
 - ¹⁰ R. Tomasello, E. Martinez, R. Zivieri, L. Torres, M. Carpentieri, and G. Finocchio, Sci. Rep. **4**, 6784 (2015).
 - ¹¹ H. Vakili, M. N. Sakib, S. Ganguly, M. Stan, M. W. Daniels, A. Madhavan, M. D. Stiles, and A. W. Ghosh, arXiv:2005.10704.
 - ¹² X. Zhang, M. Ezawa, and Y. Zhou, Sci. Rep. **5**, 9400 (2015).
 - ¹³ C. Reichhardt, D. Ray, and C. J. Olson Reichhardt, Phys. Rev. Lett. **114**, 217202 (2015).
 - ¹⁴ C. Reichhardt and C. J. O. Reichhardt, New J. Phys. **18**, 095005 (2016).
 - ¹⁵ S. A. Díaz, C. Reichhardt, D. P. Arovas, A. Saxena, and C. J. O. Reichhardt, Phys. Rev. B **96**, 085106 (2017).
 - ¹⁶ W. Jiang, X. Zhang, G. Yu, W. Zhang, X. Wang, M.B. Jungfleisch, J.E. Pearson, X. Cheng, O. Heinonen, K. L. Wang, Y. Zhou, A. Hoffmann, and S.G.E. te Velthuis, Nat. Phys. **13**, 162 (2017).
 - ¹⁷ K. Litzius, I. Lemesch, B. Krüger, P. Bassirian, L. Caretta, K. Richter, F. Büttner, K. Sato, O.A. Tretiakov, J. Förster, R.M. Reeve, M. Weigand, I. Bykova, H. Stoll, G. Schütz, G.S.D. Beach, and M. Kläui, Nat. Phys. **13**, 170 (2017).
 - ¹⁸ R. Juge, S.-G. Je, D. de Souza Chaves, L. D. Buda-Prejbeanu, J. Peña-Garcia, J. Nath, I. M. Miron, K. G. Rana, L. Aballe, M. Foerster, F. Genuzio, T. O. Menteş, A. Locatelli, F. Maccherozzi, S. S. Dhesi, M. Belmeguenai, Y. Roussigné, S. Auffret, S. Pizzini, G. Gaudin, J. Vogel, and O. Boulle, Phys. Rev. Applied **12**, 044007 (2019).
 - ¹⁹ N. P. Vizarim, C. J. O. Reichhardt, P. A. Venegas, and C. Reichhardt, arXiv: 2003.05972.
 - ²⁰ S. A. Díaz, C. Reichhardt, D. P. Arovas, A. Saxena, and C. J. O. Reichhardt, Phys. Rev. Lett. **120**, 117203 (2018).
 - ²¹ A. F. Schäffer, L. Rózsa, J. Berakdar, E. Y. Vedmedenko, and R. Wiesendanger, Commun. Phys. **2**, 27 (2019).
 - ²² C. Reichhardt, D. Ray, and C. J. O. Reichhardt, Phys. Rev. B **98**, 134418 (2018).
 - ²³ B. L. Brown, C. Reichhardt, and C. J. O. Reichhardt, New J. Phys. **21**, 013001 (2019).
 - ²⁴ C. Reichhardt and C. J. O. Reichhardt, Phys. Rev. B **101**, 054423 (2020).
 - ²⁵ C. J. O. Reichhardt and C. Reichhardt, Phys. Rev. E **99**, 012606 (2019).

- ²⁶ T.-H. Kim, H. Zhao, B. Xu, B. A. Jensen, A. H. King, M. J. Kramer, C. Nan, L. Ke, and L. Zhou, arXiv:1912.03226 and Nano Letters in press.
- ²⁷ H. Nakajima, A. Kotani, M. Mochizuki, K. Harada, and S. Mori, Appl. Phys. Lett. **111**, 192401 (2017).
- ²⁸ T. Sato, W. Koshibae, A. Kikkawa, T. Yokouchi, H. Oike, Y. Taguchi, N. Nagaosa, Y. Tokura, and F. Kagawa, Phys. Rev. B **100**, 094410 (2019).
- ²⁹ J. Miltat, S. Rohat, and A. Thiaville, Phys. Rev. B **97**, 214426 (2018).
- ³⁰ L. Zhao, Z. Wang, X. Zhang, J. Xia, K. Wu, H.-A. Zhou, Y. Dong, G. Yu, K. L. Wang, X. Liu, Y. Zhou, and W. Jiang, arXiv:1901.08206.
- ³¹ T. Nozaki, Y. Jibiki, M. Goto, E. Tamura, T. Nozaki, H. Kubota, A. Fukushima, S. Yuasa, and Y. Suzuki, Appl. Phys. Lett. **114**, 012402 (2019).
- ³² B. L. Brown, U. C. Täuber, and M. Pleimling, Phys. Rev. B **97**, 020405(R) (2018).
- ³³ B. L. Brown, U. C. Täuber, and M. Pleimling, Phys. Rev. B **100**, 024410 (2019).
- ³⁴ J. Zázvorka, F. Dittrich, Y. Ge, N. Kerber, K. Raab, T. Winkler, K. Litzius, M. Veis, P. Virnau, and M. Kläui, arXiv:2004.09244.
- ³⁵ Y.-H. Liu and Y.-Q. Li, J. Phys.: Condens. Matter **25**, 076005 (2013).
- ³⁶ J. Iwasaki, M. Mochizuki, and N. Nagaosa, Nat. Commun. **4**, 1463 (2013).
- ³⁷ J. Sampaio, V. Cros, S. Rohart, A. Thiaville, and A. Fert, Nat. Nanotechnol. **8**, 939 (2013).
- ³⁸ J. Müller and A. Rosch, Phys. Rev. B **91**, 054410 (2015).
- ³⁹ J.-V. Kim and M.-W. Yoo, Appl. Phys. Lett. **110**, 132404 (2017).
- ⁴⁰ W. Legrand, D. Maccariello, N. Reyren, K. Garcia, C. Moutafis, C. Moreau-Luchaire, S. Collin, K. Bouzehouane, V. Cros, and A. Fert, Nano Lett. **17**, 2703 (2017).
- ⁴¹ S. Hoshino and N. Nagaosa, Phys. Rev. B **97**, 024413 (2018).
- ⁴² S.-Z. Lin, C. Reichhardt, C. D. Batista and A. Saxena, Phys. Rev. B **87**, 214419 (2013).
- ⁴³ S. Pöllath, J. Wild, L. Heinen, T. N. G. Meier, M. Kronseder, L. Tutsch, A. Bauer, H. Berger, C. Pfleiderer, J. Zweck, A. Rosch, and C. H. Back, Phys. Rev. Lett. **118**, 207205 (2017).
- ⁴⁴ A. A. Thiele, Phys. Rev. Lett. **30**, 230 (1973).
- ⁴⁵ C. Reichhardt, D. Ray, and C. J. Olson Reichhardt, Phys. Rev. Lett. **114**, 217202 (2015).
- ⁴⁶ M. Henkel and M. Pleimling, *Non-Equilibrium Phase Transitions, Volume 2: Ageing and Dynamic Scaling Far From Equilibrium* (Springer, Heidelberg, 2010).
- ⁴⁷ N. N. Taleb, arXiv:2001.10488.